PHYSICAL REVIEW B **69**, 161101(R) (2004)

Charge fluctuations and electron-phonon interaction in the finite-U Hubbard model

E. Cappelluti,[1,2,*] B. Cerruti,[2] and L. Pietronero[2]

[1]*"Enrico Fermi" Research Center, c/o Compendio del Viminale, v. Panisperna 89/a, 00184 Roma, Italy*

[2]*Dipart. di Fisica, Università di Roma "La Sapienza," P. le A. Moro, 2, 00185 Roma, and INFM UdR Roma1, Italy*

(Received 29 December 2003; revised manuscript received 18 February 2004; published 15 April 2004)

In this paper we employ a Gaussian expansion within the finite-U slave-bosons formalism to investigate the momentum structure of the electron-phonon vertex function in the Hubbard model as function of U and n. The suppression of large momentum scattering and the onset of a small-$\mathbf{q}$ peak structure, parametrized by a cut-off q_c, are shown to be essentially ruled by the band narrowing factor Z_{MF} due to the electronic correlation. A phase diagram of Z_{MF} and q_c in the whole $U-n$ space is presented. Our results are in more than qualitative agreement with a recent numerical analysis and permit one to understand some anomalous features of the quantum Monte Carlo data.

DOI: 10.1103/PhysRevB.69.161101 PACS number(s): 71.10.Fd, 71.27.+a, 71.45.Lr

In the past months a variety of experiments have pointed out an important role of the electron-phonon (el-ph) interaction in many physical properties of the cuprates.[1–3] These recent findings have triggered a renewed interest for a theoretical understanding of the el-ph properties in strongly correlated systems.

One of the most remarkable effects of the strong electronic correlation on the el-ph properties is to favor forward (small $\mathbf{q}$) scattering in the electron-phonon vertex, $\mathbf{q}$ being the exchanged phonon momentum. This feature was investigated in the past by means of analytical techniques based on slave-bosons or X operators.[4–8] The assumption of forward scattering predominance within an el-ph framework was shown to explain in a natural way several anomalous properties of cuprates as the difference between transport and superconducting el-ph coupling constants,[6,7] the linear temperature behavior of the resistivity,[9] the d-wave symmetry of the superconducting gap.[8,10] Small $\mathbf{q}$ scattering selection was shown moreover to be responsible in a natural way for high-T_c superconductivity within the context of the nonadiabatic superconductivity.[11] Microscopic models based on small-$\mathbf{q}$ or, equivalently, on long-range electron interactions were also proposed to account for the anomalous kink in the photoemission data.[12,13]

So far, this important feature has been analyzed only by means of analytical approaches in the $U=\infty$ limit and a definitive confirmation of it based on numerical methods was lacking. The charge response at finite U was addressed in Refs. 14 and 15, which however focused only on $\mathbf{q}=0$ susceptibilities. With these motivations in a recent paper Huang *et al.* have addressed this issue in the two-dimensional Hubbard model with generic U by using quantum Monte Carlo (QMC) techniques on an 8×8 cluster.[16] Their results provide a good agreement with the previous analytical studies and represent an important contribution to assess the relevance of el-ph interaction in correlated system.

In this paper we employ the slave-boson techniques to investigate the evaluation of the momentum structure of the el-ph vertex interaction as function of the Hubbard repulsion U. While the previous analytical studies were limited to the $U=\infty$ limit,[4–8] we were able in this way to evaluate the small momenta selection in the whole phase diagram of parameters $U-n$, where n is the electron filling. In particular we show that the predominance of small $\mathbf{q}$ scattering is strongly dependent on the closeness of the system to the metal-insulator transition (MIT). Our analysis suggests that forward scattering is essentially ruled by the one-particle (mean-field) parameter Z_{MF}, which represents the band narrowing factor due to the correlation effects. We also discuss some anomalous features of the numerical results of Ref. 16. The fair agreement between our slave-boson results and the quantum Monte Carlo data[16] supports the reliability of our approach to investigate these issues. Note that, while the present study is mainly focused on charge (el-ph) fluctuations, a similar approach could be used to investigate spin correlations and magnetic instabilities. Previous studies at finite U were indeed limited at $\mathbf{q}=(0,0)$ and $\mathbf{q}=(\pi,\pi)$.[4,14,15,17] The analysis of the full momentum structure of the spin susceptibilities in the $U-n$ phase diagram will be the object of a future publication.

The working tool of this paper will be the four slave-boson method first introduced by Kotliar and Ruckenstein to investigate the Hubbard model at finite U. In this approach the physical Hilbert space is enlarged by introducing, in addition to the standard fermionic degrees of freedom $c_{i\sigma}$, four auxiliary bosons, e, d, p_σ, which count, respectively, empty, double, and single occupied (with spin σ) sites.[17] The extended Hilbert space is thus restricted to the physical one by the Lagrange multipliers $\lambda^{(1)}$, $\lambda^{(2)}_\sigma$. The Hubbard Hamiltonian reads thus:

$$H=\sum_{ij\sigma} Z_{ij\sigma}[e,d,p_\sigma,p_{-\sigma}]t_{ij}c^\dagger_{i\sigma}c_{j\sigma} + \sum_i \lambda^{(1)}_i\left[e^\dagger_i e_i+\sum_\sigma p^\dagger_{i\sigma}p_{i\sigma}+d^\dagger_i d_i-1\right] + \sum_{i\sigma}\lambda^{(2)}_{i\sigma}[c^\dagger_{i\sigma}c_{i\sigma}-p^\dagger_{i\sigma}p_{i\sigma}-d^\dagger_i d_i], \quad (1)$$

where t_{ij} is the bare hopping term, here considered within a nearest neighbor model, and $Z[\ldots]$ is the reduction of the hopping term due to the correlation effects. A standard method to account for charge, spin, and different kinds of fluctuations is to expand Eq. (1) at the Gaussian level around

its mean-field solution for the auxiliary fields e, d, p_σ, $\lambda^{(1)}$, $\lambda_\sigma^{(2)}$.[14,18] Equation (1) can be thus re-written as

$$H=\sum_{\mathbf{k}\sigma}[Z_{\mathrm{MF}}t_{\mathbf{k}}+\lambda_\sigma^{(2)}]c_{\mathbf{k}\sigma}^\dagger c_{\mathbf{k}\sigma}+\sum_{\mathbf{q}\mu}\alpha_{-\mathbf{q}}^\mu[B_{\mathbf{q}}^{-1}]^{\mu\nu}\alpha_{\mathbf{q}}^\nu$$

$$+\sum_{\mathbf{kq}\sigma\mu}\Lambda_{\mathbf{k},\mathbf{q}}^\mu c_{\mathbf{k}+\mathbf{q}\sigma}^\dagger c_{\mathbf{k}\sigma}\alpha_{\mathbf{q}}^\mu+\mathrm{const.},\qquad(2)$$

where the first term describes the mean-field approximation where all the auxiliary fields are determined by their self-consistent saddle point solution, the second term is the quadratic fluctuations of the auxiliary fields about their mean-field solution, comprehensive of the electronic loop self-energy contributions,[14,18] and the third one is the linear electron-slave-boson interaction. The index μ, ν runs on the seven auxiliary fields. Explicit expressions for the slave-boson matrix dispersion $[B_{\mathbf{q}}^{-1}]^{\mu\nu}$ and the electron-slave-boson matrix elements $\Lambda_{\mathbf{k},\mathbf{q}}^\mu$ could be found in Ref. 14.

The el-ph vertex function $g(\mathbf{k},\mathbf{q},\omega)$ in the presence of electronic correlation can be promptly determined as the linear response of the systems described by Eq. (2) to an external charge excitation. In the paramagnetic case the spin index σ can be dropped and the auxiliary field space reduced to five components. At the Gaussian level we have[14,18]

$$g(\mathbf{k},\mathbf{q};\omega)=1-2\sum_{\mu\nu}\Lambda_{\mathbf{k},\mathbf{q}}^\mu[D_{\mathbf{q}}^{-1}(\omega)]^{\mu\nu}\tilde{\Pi}_{\mathbf{q}}^\nu(\omega),\qquad(3)$$

where the factor 2 takes into account the spin degeneracy, D^{-1} is the renormalized slave-boson propagator, $2[D_{\mathbf{q}}^{-1}(\omega)]^{\mu\nu}=2[B_{\mathbf{q}}^{-1}]^{\mu\nu}+\Pi_{\mathbf{q}}^{\mu\nu}(\omega)$, which includes the "bubble" contribution to the slave-boson self-energy

$$\Pi_{\mathbf{q}}^{\mu\nu}(\omega)=\sum_{\mathbf{k}}\Lambda_{\mathbf{k},\mathbf{q}}^\mu\Lambda_{\mathbf{k},\mathbf{q}}^\nu\frac{f(E_{\mathbf{k}})-f(E_{\mathbf{k}+\mathbf{q}})}{E_{\mathbf{k}+\mathbf{q}}-E_{\mathbf{k}}-\omega},\qquad(4)$$

and where

$$\tilde{\Pi}_{\mathbf{q}}^\nu(\omega)=\sum_{\mathbf{k}}\Lambda_{\mathbf{k},\mathbf{q}}^\nu\frac{f(E_{\mathbf{k}})-f(E_{\mathbf{k}+\mathbf{q}})}{E_{\mathbf{k}+\mathbf{q}}-E_{\mathbf{k}}-\omega}.\qquad(5)$$

Here $f(x)$ is the Fermi factor and $E_{\mathbf{k}}$ is the renormalized electronic dispersion $E_{\mathbf{k}}=Z_{\mathrm{MF}}t_{\mathbf{k}}$.

We are now in the position to apply Eqs. (3)–(5) to calculate the **q** structure of the electron-phonon vertex function in the presence of electronic correlation for generic Hubbard repulsion U and electron filling n. From the technical point of view we use a slightly different version of the four-slave-boson technique as introduced by Kotliar and Ruckenstein. We note indeed that Eq. (2), when derived in the context of the Kotliar–Ruckenstein formalism, presents serious pathologies at finite U in the limit $n\to 0,2$ where the linear electron-slave-boson matrix elements diverge.[19] As pointed out in Ref. 17, however, several choices for the auxiliary fields e, d, p_σ can be employed as long as they fulfill the constraints imposed by the real Hilbert space. We make use of this freedom to avoid those unphysical divergences. The analytical derivation of Eq. (2) in this new basis of auxiliary fields is long and cumbersome, but quite straightforward and it does not affect in a significant way our results which focus on the MIT transition. Technical details will thus be presented in a longer publication.

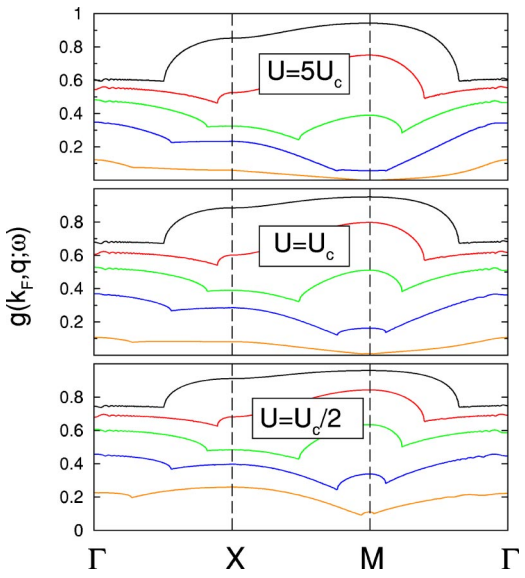

FIG. 1. (Color online) Momentum dependence of the electron-phonon vertex function $g(k_F,\mathbf{q};\omega=0)$ in the presence of electronic correlation for different U/U_c and n. In each panel solid lines represent, from the top to the bottom: $n=0.1,0.3,0.5,0.7,0.9$. Standard labels for the high symmetry points correspond to $\Gamma=(0,0)$, $X=(0,\pi)$, $M=(\pi,\pi)$.

In Fig. 1 we plot the evolution of momentum structure of the electron-phonon vertex function $g(k_F,\mathbf{q};\omega=0)$ for $\omega=0$ and $\mathbf{k}=k_F$ lying on the Fermi surface for different electron filling n and U. The top panel in Fig. 1 reproduces the n-dependence of $g(k_F,\mathbf{q};\omega=0)$ in the large-U limit. It agrees quite well with the previous studies of Refs. 6–8 and it shows the suppression of the large-**q** scattering as the MIT is approached for $n\to 1$ and the corresponding development of a small-**q** momentum structure. As a marginal difference we can note that the four-slave-boson approach at finite U predicts a less pronounced peaked structure than the $U=\infty$ one-slave-boson method. This slight discrepancy can be traced back to the different band narrowing factor between our case $[Z_{\mathrm{MF}}\sim 2\delta/(1+\delta)$ as in Ref. 17] and the one-slave-boson $U=\infty$ treatment ($Z_{\mathrm{MF}}\sim\delta$).

One of the main results of our analysis is that it permits one to investigate the MIT and the momentum structure of the el-ph vertex along a different path, namely increasing U for *fixed* n. As shown by the comparison between the three panels of Fig. 1, the predominance of forward scattering is effectively suppressed as long as we move far from the MIT by reducing the Hubbard repulsion U, in a similar way with what is found as function of n. This observation suggests that the small-**q** structure is only ruled by some macroscopic parameter which quantifies the closeness to the metal-insulator transition, regardless of the microscopic parameters as U or n. A natural candidate along this perspective is the band narrowing Z_{MF}, which vanishes $Z_{\mathrm{MF}}\to 0$ at the MIT ($n=1$, $U\geqslant U_c$) and $Z_{\mathrm{MF}}\to 1$ in the uncorrelated limit ($n=0,2$ or $U=0$).

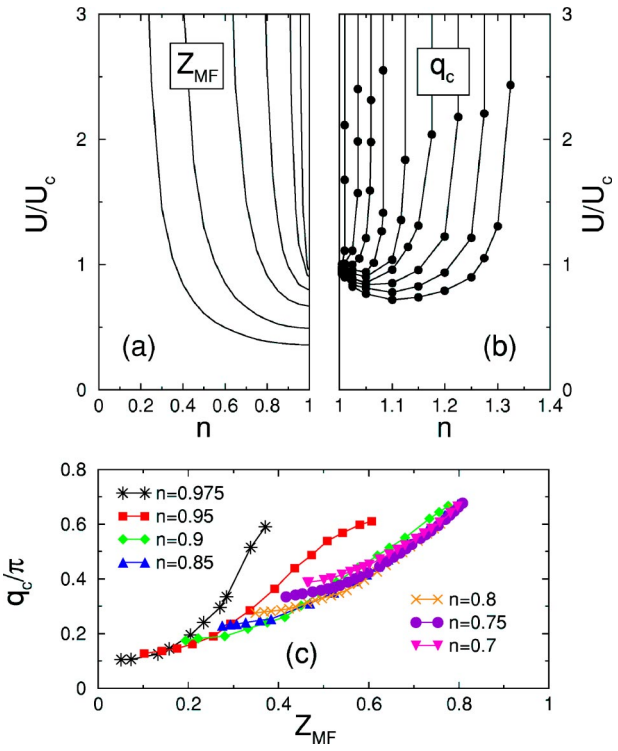

FIG. 2. (Color online) Plot of the isolines for the quantities Z_{MF} (a) and q_c (b) in the $U-n$ space. Since both quantities are symmetric for reflection with respect to the $n=2$ axis, they are shown, respectively, in just one half-plane. Solid lines are [(a), from right to the left]: $Z_{\mathrm{MF}}=0.1,0.2,0.4,0.6,0.8,0.9$; [(b), from left to right]: $q_c=0.2,0.3,0.4,0.5,0.6,0.8,1.0,1.2,1.4$. (c) Plot of q_c vs Z_{MF} for different electron filling n.

The effectiveness of the electronic correlation in giving rise to a small-**q** structure in the electron-phonon scattering has been previously discussed in literature in terms of a cut-off parameter q_c.[11] On the physical ground q_c is expected to be related to the inverse of the correlation length ξ, $q_c \propto 1/\xi$. At the MIT, $\xi\rightarrow\infty$ and $q_c\rightarrow 0$. For practical purposes, it is often difficult to extract a cut-off parameter q_c from a complex structure as those shown in Fig. 1. To this aim we define a cut-off q_c as the full width at the half maximum (FWHM) of the electron-phonon vertex $|g(k_F,\mathbf{q};\omega=0)|^2$ along the Γ-M line with respect to its $\mathbf{q}=0$ value. We would like to stress that this definition of q_c is just one of the possible choices and it does not pretend to be rigorous. As a matter of fact for systems far from the MIT, where no well-defined $\mathbf{q}=0$ peak is recovered, no q_c according to such a definition can be found. This should be interpreted as the absence of significant small-**q** modulations induced by the electronic correlation. Note, on the other hand, that close to the MIT the small-**q** peak can always be approximated as a Lorentzian, and the definition of q_c introduced earlier is indeed directly related to the inverse of the correlation length ξ.

In Figs. 2(a) and 2(b) we plot the Z_{MF} and q_c isolines as obtained by applying our FWHM definition in the whole $U-n$ phase diagram. The striking similarities between panels (a) and (b) confirm that the small-**q** structure is mainly ruled by the strong band narrowing close to the MIT. This is pointed out in the most remarkable way in panel (c) where the cut-off q_c, evaluated for different n and different U, is shown to lie on an almost universal curve when plotted as function of Z_{MF}. This is a quite important result because the band narrowing factor Z_{MF}, as well as quasiparticle spectral weight Z_{QP} which is strongly related to Z_{MF}, is in principle a physical quantity which can be experimentally determined to provide an estimate of q_c. The universality of q_c as function of Z_{MF} also points toward some general mechanism responsible for the small-**q** scattering. This mechanism has been discussed in literature in terms of proximity to a phase separation which is reflected in a charge response instability at $\mathbf{q}=0$. Before addressing the connection between small-**q** scattering and phase separation, we would note however that, although the universal behavior of q_c vs Z_{MF} appears quite robust, some discrepancies appear for values of n very close to $n=1$. This is also in agreement with a comparison between panels (a) and (b), which shows that for $n=1$, in contrast to the Z_{MF} isolines, all the q_c curves converge to the $U=U_c$ point, where q_c jumps from $q_c=\pi$ to $q_c=0$ from $U=U_c^-$ to $U=U_c^+$. A closer look at this discrepancy shows that it can be related to the presence of the Van Hove singularity at $n=1$. Indeed, while the quantity Z_{MF} does not depend on the details of the electronic dispersion, in this case the $\mathbf{q}=0$ response functions are described by an ideal metal with *infinite* density of states for any $U\leqslant U_c^-$. It can be checked that the introduction of a finite t' removes this anomalous feature and q_c evolves in a smooth way increasing U from $U=0$ to $U=U_c$ for $n=1$.

As a final issue of this letter we would like to comment on the robustness of our results, based on a Gaussian expansion within the context of a finite-U slave-boson formalism, with respect to the inclusion of higher order terms. A good check in this perspective would be the comparison of our data with **q**-resolved numerical calculations. Unfortunately, simulation and numerical work along this line is lacking in the literature since the widely diffuse dynamical mean-field approach mainly probes only local (-integrated) quantities whereas exact diagonalization and QMC techniques are limited by finite size of the cluster and by finite temperature effects. A seminal step to fill the gap has been provided by Huang *et al.*, who provided in Ref. 16, for the first time to our knowledge, numerical support by QMC simulations for the insurgence of small-**q** structure in the el-ph vertex function by increasing U. As a by-product of their analysis, Huang *et al.* also reported an interesting increasing of the absolute magnitude of the el-ph vertex function for small momentum $\mathbf{q}=(\pi/4,\pi/4)$ in the large U regime, whereas the increase is absent for large momentum $\mathbf{q}=(\pi,\pi)$. This is quite puzzling because the development of a small-**q** structure is thought to be relative to the large momentum scattering and it is usually not accompanied by an increase of the magnitude of g at $\mathbf{q}=0$. The origin of this anomalous feature has been not well understood so far and a possible connection with charge excitations driven by the exchange term $J\propto t^2/U$ in the large U limit was mentioned.[16]

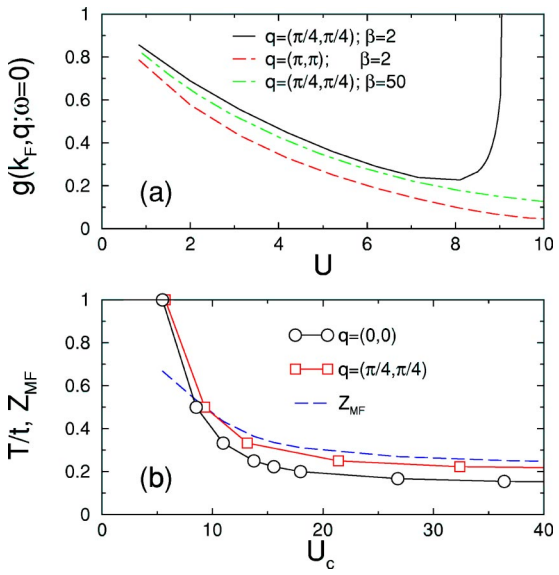

FIG. 3. (Color online) (a) Dependence of the el-ph vertex function on U for $n=0.88$ and for $\mathbf{q}=(\pi/4,\pi/4)$ (solid line, $\beta=2$), $\mathbf{q}=(\pi,\pi)$ (dashed line, $\beta=2$), and $\mathbf{q}=(\pi/4,\pi/4)$ (dot-dashed line, $\beta=50$). (b) Phase diagram for phase separation ($\mathbf{q}=0$) and charge instability ($\mathbf{q}=\pi/4,\pi/4$). The dashed line shows the factor Z_{MF} evaluated along the phase separation instability line.

In order to test the reliability of our results we have addressed this issue within the context of our slave-boson formalism. In Fig. 3(a) we show the dependence of the el-ph vertex function $g(k_F,\mathbf{q};\omega=0)$ on the Hubbard repulsion U as calculated within our approach for the same parameters as in Ref. 16, namely $n=0.88$, $\mathbf{q}=(\pi/4,\pi/4)$, $\mathbf{q}=(\pi,\pi)$, $\beta=2$, where β is the inverse of the temperature T in units of the nearest-neighbor hopping element t. The agreement between our findings and the data of Ref. 16 is quite excellent, although quantitative differences are of course present. In particular we find that, while for large momenta $g(k_F,\mathbf{q};\omega=0)$ steadily decreases with U, for $\mathbf{q}=(\pi/4,\pi/4)$ it shows an upturn for $U\simeq 8$ until a divergence occurs for $U_c\simeq 9.3$, signaling a charge instability.[20] According to this view one is tempted to associate the upturn of the el-ph vertex function $g(k_F,\mathbf{q};\omega=0)$ as a function of U reported in Ref. 16 as an incipient transition toward some charge instability or phase separation.[21] This does not imply however that phase separation is effectively established, and it should be remarked that the actual occurrence of phase separation in the Hubbard model is still an object of debate.[22] In particular the large temperature $\beta=2$ at which the QMC were performed could play a crucial role in that. To investigate this final issue we again evaluated the el-ph vertex function for the same parameters but at a much lower temperature $\beta=50$. As shown in Fig. 3(a), it is quite surprising that the charge instability disappears when decreasing the temperature.

In order to understand in more detail the origin of the phase separation instability as function of the temperature T we show in Fig. 3(b) the phase diagram in the T vs U space with respect to phase separation ($\mathbf{q}=0$) and to charge ordering ($\mathbf{q}=(\pi/4,\pi/4)$). Phase separation as well as charge instabilities occur in our slave-boson calculations only above a certain temperature $T/t\gtrsim 0.2$ ($\beta\lesssim 5$). An interesting insight comes from the comparison of the critical temperature T_c at which the instability toward phase separation occurs with the band narrowing factor Z_{MF} (Fig. 3). The similar dependence of T_c and Z_{MF} on U points out that the onset of phase separation by increasing temperature is ruled by the comparison between the temperature T and the effective bandwidth $W=Z_{\mathrm{MF}}8t$ energy scales. In particular phase separation is established when T becomes of the same order of $Z_{\mathrm{MF}}t$. We would like to stress that in principle the phase separation instability found by our slave-boson calculations could be washed out when higher order fluctuations than the Gaussian ones are taken into account. The agreement between our data and QMC results suggests however that the correlation between small-$\mathbf{q}$ modulation, phase separation, and the upturn as function of U could be a robust feature of correlated systems. At a speculative level, we think that the small coherent part of the electronic spectral weight (with the electronic dispersion scaling with Z_{MF}) could be responsible for the tendency toward phase separation, which is however prevented by the presence of the incoherent states. Further analytical and numerical work on this direction will help to shed new light on this issue.

*Email address: emmcapp@romal.infn.it

[1] A. Lanzara *et al.*, Nature (London) **412**, 510 (2001).
[2] See H. Keller, Physica B **326**, 283 (2003).
[3] M. d'Astuto *et al.*, Phys. Rev. Lett. **88**, 167002 (2002).
[4] J.H. Kim and Z. Tesanovic, Phys. Rev. Lett. **71**, 4218 (1993).
[5] M. Grilli and C. Castellani, Phys. Rev. B **50**, 16880 (1994).
[6] M.L. Kulić and R. Zeyher, Phys. Rev. B **49**, 4395 (1994).
[7] R. Zeyher and M.L. Kulić, Phys. Rev. B **53**, 2850 (1996).
[8] M.L. Kulić, Phys. Rep. **338**, 1 (2000).
[9] E. Cappelluti and L. Pietronero, Europhys. Lett. **36**, 619 (1996).
[10] P. Paci *et al.*, Eur. Phys. J. B **17**, 235 (2000).
[11] C. Grimaldi *et al.*, Phys. Rev. Lett. **75**, 1158 (1995).
[12] M.L. Kulić and O.V. Dolgov, cond-mat/0308597 (unpublished).
[13] Z.-X. Shen, Proceedings of the VII International Conference on High-T_c Superconductors, Rio de Janeiro, 2003, Physica C (to be published).
[14] M. Lavagna, Phys. Rev. B **41**, 142 (1990).
[15] H. Kaga, Phys. Rev. B **46**, 1979 (1992).
[16] Z.B. Huang, W. Hanke, E. Arrigoni, and D.J. Scalapino, Phys. Rev. B **68**, 220507 (2003).
[17] G. Kotliar and A.E. Ruckenstein, Phys. Rev. Lett. **57**, 1362 (1986).
[18] F. Becca *et al.*, Phys. Rev. B **54**, 12443 (1996).
[19] B. Cerruti, Diploma thesis, University of Rome "La Sapienza," 2003.
[20] B. Cerruti, E. Cappelluti, and L. Pietronero, cond-mat/0307190 (unpublished).
[21] Investigation of a phase separation instability was prevented in Ref. 16 due to the momentum discretization due to the finite cluster.
[22] See for instance F. Becca, M. Capone, and S. Sorella, Phys. Rev. B **62**, 12700 (2000), and references therein.